Available online at www.sciencedirect.com
SCIENCE DIRECT®
International Journal of Heat and Mass Transfer 48 (2005) 1361–1372
International Journal of HEAT and MASS TRANSFER
www.elsevier.com/locate/ijhmt

Natural convection in an enclosure with disconnected and conducting solid blocks

Ali A. Merrikh [a], José L. Lage [b,*]

[a] Department of Internal Medicine, University of Texas, Southwestern Medical Center at Dallas, Dallas, TX 75390-9034, USA
[b] Laboratory for Porous Materials Applications, Mechanical Engineering Department, Southern Methodist University, Dallas, TX 75275-0337, USA

Received 24 June 2004; received in revised form 25 September 2004
Available online 8 December 2004

Abstract

Natural convection through a rectangular enclosure filled with a fluid bathing several discrete, conducting and disconnected solid objects is common in many applications, such as environmental control (e.g., indoor buildings, storage), materials processing (e.g., drying), food processing (e.g., baking), and electronics (e.g., cabinets). The case of an enclosure heated from the side and containing equally spaced, conducting solid square blocks is investigated here by using a continuum model, which treats the fluid and solid constituents individually. The dispersive effect of the solid constituent is isolated by increasing the number of solid blocks (N) while reducing their size as to maintain their relative total volume constant. Results obtained for a wide Rayleigh number (Ra) range and several values of solid-to-fluid conductivity ratio (κ) show the strong hindrance effect of the blocks on the convection process to be dependent on a minimum number of blocks, $N_{\min}$, for every Ra. An analytical expression predicting $N_{\min}$ is proposed and validated by the numerical results.

1. Introduction

The study of transport phenomena in heterogeneous media is fundamental for the design and optimization of several devices and processes, including filters and catalytic reactors, human respiration and capillary circulation, underground contaminant transport, oil and gas exploration and extraction, materials processing (e.g., casting, sintering, etching), heat exchangers (e.g., porous-enhanced), grain storage, food processing, and many others. Common to these devices and processes is the existence of at least two constituents, a solid and a fluid, that would characterize the media as heterogeneous.

A very important common characteristic of solid–fluid heterogeneous media is the very complex interface morphology of the constituents whose complexity translates itself into a formidable obstacle for detailed numerical simulations. Because of the tremendous computational effort required to map the solid–fluid interface and hence to resolve discontinuity in physical properties across the interfaces, simulation of such phenomena has been a challenge. This aspect might explain the dwarf of studies in this particular area.

The case of a fluid saturated rectangular enclosure heated from the side containing several equally spaced conducting and disconnected solid square blocks, as

* Corresponding author. Tel.: +1 214 768 2361; fax: +1 214 768 4173.
E-mail address: jll@engr.smu.edu (J.L. Lage).

0017-9310/$ - see front matter © 2004 Elsevier Ltd. All rights reserved.
doi:10.1016/j.ijheatmasstransfer.2004.09.043

Nomenclature

A	enclosure aspect ratio
d	block side-length, m
D	non-dimensional block side-length
g	gravitational acceleration, m^2/s
H	enclosure height, m
$\mathbf{i},\mathbf{j}$	unit vectors in the x- and y-direction
k	thermal conductivity, W/mK
L	enclosure length, m
N	number of solid blocks inside the enclosure
N_{min}	minimum number of solid obstacles necessary for flow switch, Eq. (14)
Nu	Nusselt number
Pr	Prandtl number
p	pressure, Pa
P	non-dimensional pressure
Ra	Rayleigh number
S	non-dimensional distance between wall and blocks
t	time, s
T	temperature, K
u	velocity component in the x-direction, m/s
U	x-direction non-dimensional velocity component
v	velocity component in the y-direction, m/s
$\mathbf{v}$	velocity vector
V	y-direction non-dimensional velocity component
$\mathbf{V}$	non-dimensional velocity vector
x,y	horizontal and vertical Cartesian coordinates, m

Greek symbols

α	thermal diffusivity, m^2/s
β	isobaric coefficient of volumetric thermal expansion, 1/K
γ	solid-to-fluid volume ratio within the enclosure
η	y-direction non-dimensional coordinate
κ	solid-to-fluid conductivity ratio
μ	dynamic viscosity, kg/ms
ν	kinematic viscosity, m^2/s
θ	non-dimensional temperature
ρ	density, kg/m^3
σ	thermal capacity ratio
τ	non-dimensional time
ξ	x-direction non-dimensional coordinate

Subscripts

av	average
c	cold
f	fluid
h	hot
m	mid-plane
s	solid

sown schematically in Fig. 1, is investigated here. This configuration is common in many engineering applications such as environmental control (e.g., indoor buildings, storage), materials processing (e.g., drying), food processing (e.g., baking), and electronics (e.g., cabinets).

Although heterogeneous, the medium configuration considered here has relatively simple interface morphology. Hence, the problem lends itself to a continuum model, which treats the fluid and solid constituents individually. This higher resolution treatment, in which continuum transport equations (such as the Navier–Stokes equations for the transport of momentum within the fluid constituent) are used within each constituent individually, requires solid–fluid interface mapping.

The main advantage of a continuum model approach when modeling transport in heterogeneous media is the detailed information obtained by the model. The drawback is the need for locating and mapping the constituent interfaces, and for the strong numerical effort required solving the equations when the internal geometry (solid–fluid interface) is not simple.

The objective here is to investigate the effect of the solid obstacles on the heat transfer process by changing the number and size of the solid obstacles inside an enclosure. As such, the internal structure of the medium can

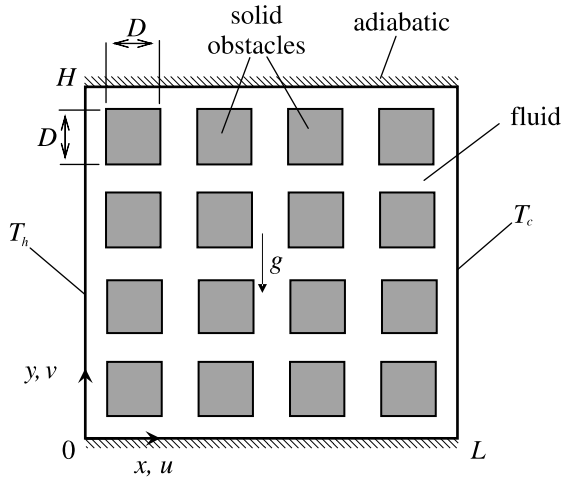

Fig. 1. Schematic of the heterogeneous enclosure, with fluid and solid constituents, and the boundary conditions.

be made more or less geometrically complex, altering the efficiency of the model when it comes to computational effort. To isolate other possible effects, the total heat and mass capacity of the solid constituent is kept constant. This work is directly related to previous studies by Merrikh and Mohamad [1] which considered conducting obstacles in an enclosure of aspect ratio 2, and by Merrikh et al. [2], which considered heat transfer within a fluid filled enclosure with thermal energy being generated by discrete, disconnected solid obstacles.

2. Continuum model equations and boundary conditions

Fig. 1 presents a sketch of the domain, as seen at the continuum visual resolution, consisting of a fluid filled enclosure containing several conducting solid obstacles that are disconnected and distributed uniformly within the enclosure. The enclosure is subjected to a horizontal temperature difference (applied at the walls), which in turn induces natural convection by the fluid within the domain.

In the present study, the medium is composed of two distinct, homogeneous and isotropic constituents, namely the fluid and solid, within the enclosure. Transport equations for each constituent together with appropriate compatibility conditions at their interfaces (also referred to as "internal" boundary conditions) are discussed next. For the fluid with constant properties, the continuum transport equations are the continuity, momentum and energy equations, respectively:

$$\nabla \cdot \mathbf{v} = 0 \tag{1}$$

$$\rho_f \left[\frac{\partial \mathbf{v}}{\partial t} + (\mathbf{v}\cdot\nabla)\mathbf{v}\right] = -\nabla p + \mu\nabla^2\mathbf{v} + \rho_f g\beta(T - T_c)\mathbf{j} \tag{2}$$

$$(\rho c)_f \left(\frac{\partial T}{\partial t} + \mathbf{v}\cdot\nabla T\right) = k_f \nabla^2 T \tag{3}$$

The solid obstacles within the enclosure participate, indirectly, amid the transport of momentum by the fluid through their solid–fluid interfaces where the no-slip condition is imposed. Their participation on the energy transport across the enclosure, however, is expected to be more effective for being conducting solids. The energy balance equation, valid for the solid blocks, is

$$(\rho c)_s \frac{\partial T}{\partial t} = k_s \nabla^2 T \tag{4}$$

The fluid density variation in the buoyancy term of Eq. (2) is modeled using the classical Oberbeck–Boussinesq approximation with T_c being the reference fluid temperature.

For solving Eqs. (1)–(4) the velocity components u and v are set to zero at all solid surfaces. The right wall of the enclosure is maintained at temperature T_c, and the left wall is at $T_h > T_c$. The horizontal top and bottom surfaces of the enclosure are adiabatic.

Using non-dimensional coordinates, $(\xi,\eta) = (x,y)/H$, fluid velocity, $\mathbf{V} = \mathbf{v}H/\alpha_f$, time, $\tau = t\alpha_f/H^2$ pressure, $P = pH^2/\rho_f\alpha_f^2$, and temperature, $\theta = (T - T_c)/(T_h - T_c)$, and defining dimensionless parameters such as the Prandtl number, $Pr = \nu/\alpha$, the Rayleigh number, $Ra = g\beta H^3(T_h - T_c)/\nu\alpha_f$, and fluid-to-solid thermal capacity ratio, $\sigma = (\rho c)_s/(\rho c)_f$, Eqs. (1)–(4) are converted to the following non-dimensional equations.

$$\nabla \cdot \mathbf{V} = 0 \tag{5}$$

$$\frac{\partial \mathbf{V}}{\partial \tau} + (\mathbf{V}\cdot\nabla)\mathbf{V} = \nabla P + Pr\nabla^2\mathbf{V} + Ra\,Pr\theta\mathbf{j} \tag{6}$$

$$\frac{\partial \theta}{\partial \tau} + \mathbf{V}\cdot\nabla\theta = \nabla^2\theta \tag{7}$$

$$\left(\frac{\sigma}{\kappa}\right)\frac{\partial \theta}{\partial \tau} = \nabla^2\theta \tag{8}$$

The non-dimensional mathematical representations of the boundary conditions are

$$\theta = 1,\ U = V = 0 \quad \text{at } \xi = 0;$$
$$\theta = U = V = 0 \quad \text{at } \xi = A \tag{9}$$

$$\frac{\partial \theta}{\partial \eta} = U = V = 0 \text{ at } \eta = 0 \text{ and } \eta = 1 \tag{10}$$

At the solid–fluid interfaces, the following compatibility conditions apply

$$U = V = 0; \quad \theta|_f = \theta|_s; \quad \left.\frac{\partial\theta}{\partial n}\right|_f = \kappa\left.\frac{\partial\theta}{\partial n}\right|_s \tag{11}$$

where A is the aspect ratio of the enclosure, $A = L/H$, n is the unit vector along the direction normal to each and every block boundary, and κ is the solid-to-fluid thermal conductivity ratio k_s/k_f.

In summary, the results of the continuum model depend on the following parameters: Ra, Pr, σ, κ, and the geometrical parameters A, D (the non-dimensional solid body side-length, $D = d/H$), and on the number of solid blocks inside the enclosure, N.

Heat transfer across the enclosure is evaluated using the average Nusselt number at the hot wall, defined as $Nu_{av} = h_{av}H/k_f$. Then, to evaluate Nu_{av} one must first determine the value of h_{av}, which can be obtained from the definition $h_{av} = q''_{av}/(T_h - T_c)$, which requires the determination of q''_{av}, to be found from the conduction heat flux at the hot wall, namely $q''_{av} = -k_f(\partial T/\partial x)_{av,h}$. So, the hot-wall average Nusselt number is

$$Nu_{av} = \frac{h_{av}H}{k_f} = \left(\frac{H}{T_h - T_c}\right)\left[\frac{1}{H}\int_0^H -\left.\frac{\partial T}{\partial x}\right|_{x=0} dy\right]$$
$$= -\int_0^1 \left.\frac{\partial\theta}{\partial\xi}\right|_{\xi=0} d\eta \tag{12}$$

3. Results and discussion

Although the model equations were presented in their transient form, only the steady-state solutions are presented here. Moreover, the enclosure aspect ratio is set as $A = 1$, and $Pr = 1$. The number of solid blocks N is varied from 9 to 144, while the total mass of solid block inside the enclosure is kept constant by fixing the solid-to-fluid volume ratio, γ to 36%. Although arbitrary, this solid-to-fluid volume ratio criterion that is maintained constant by reducing the size D of the blocks, facilitates the numerical modeling and provides results that are general enough for our purposes. Observe that the non-dimensional block size, D, is uniquely determined once N and γ are determined, as $D = (\gamma/N)^{0.5}$. Hence, the deciding parameters for the continuum model are limited to Ra, κ, and N. The effect of fluid and solid constituent thermal conductivity is studied by considering $\kappa = 0.1$, 1, 10, and 100, with results presented for Ra varying from 10^5 to 10^8. A summary of the parameter values used here is presented in Table 1.

Eqs. (5)–(8) of the continuum model, together with the corresponding boundary conditions, are discretized and solved using the control-volume method following SIMPLER [3] algorithm with the QUICK [4] scheme.

For the most stringent case considered here, i.e., using the maximum number of blocks, $N = 144$, and the highest Rayleigh number, $Ra = 10^8$, a uniform grid with 241×241 nodes yielded average Nusselt number results that were within 1% of the results obtained when using a 301×301 grid. Therefore, all reported results were obtained with a 241×241 grid.

The numerical approach is validated in three ways. The first considers an enclosure clear of solid bodies ($N = 0$), for which present results compare very well with the published results from several distinct sources, as shown in Table 2. The second considers the case of a single solid conducting square, located at the center of the enclosure, identical to the configuration studied by House et al. [5]. Table 3 shows the present results to compare well with the published results.

Fig. 2a exhibits streamlines obtained with $Ra = 10^6$ and $\kappa = 1$. For small number of larger blocks (e.g., $N = 9$ and 16) the flow is stronger along the heated and cooled walls. As the number of blocks increases, and their size is reduced, the flow tends to migrate away from the wall, occupying the vertical channel between the two columns of blocks adjacent to the walls. This phenomenon seems to be a response by the system to the increased flow resistance, as the blocks get closer to the solid wall. In this case, fluid prefers the less resistive path in between the two adjacent columns of blocks. A switch in flow path, observed when N grows from 16 to 36, requires the buoyancy region that propels the fluid (region affected by the heating or cooling wall) to extend itself beyond the column of blocks adjacent to the walls. The flow path switch is revealed also by the reduced flow near the top-left and bottom-right corners of the enclosure when N increases. As a consequence, the convective heat transport is expected to get hindered as well,

Table 1
Summary of parameter values used in the present study

Ra	10^5, 10^6, 10^7, 10^8
Pr	1
A	1
γ	0.36
κ	0.1, 1, 10, 100
N	9, 16, 36, 64, 144
D	0.2, 0.15, 0.1, 0.075, 0.05

Table 3
Comparison between average Nusselt numbers for a square enclosure filled fluid ($Pr = 0.71$) and a conducting square solid body at the center

Ra	D	κ	House et al. [5]	Present
10^5	0.5	0.2	4.624	4.605
10^5	0.5	5.0	4.324	4.280
10^6	0.9	0.2	2.402	2.352

Table 2
Comparison between published results and results obtained with the continuum model based on the average Nusselt number, for a square enclosure filled only with a clear fluid ($Pr = 0.71$, unless otherwise noted)

Ra	House et al. [5]	de Vahl Davis [6]	Hortmann et al. [7]	Kalita et al. [8]	Lage and Bejan [9] $Pr = 1$	Bejan[a] [10]	Present
10^4	2.254	2.243	2.244	2.245	–	2.418	2.244
10^5	4.561	4.519	4.521	4.522	4.9	4.715	4.536
10^6	8.923	8.800	8.825	8.829	9.2	9.194	8.860
10^7	–	–	–	16.52	17.9	17.927	16.625
10^8	–	–	–	–	31.8	34.954	31.200

[a] Analytical estimates obtained from Eq. (7.100), p. 369.

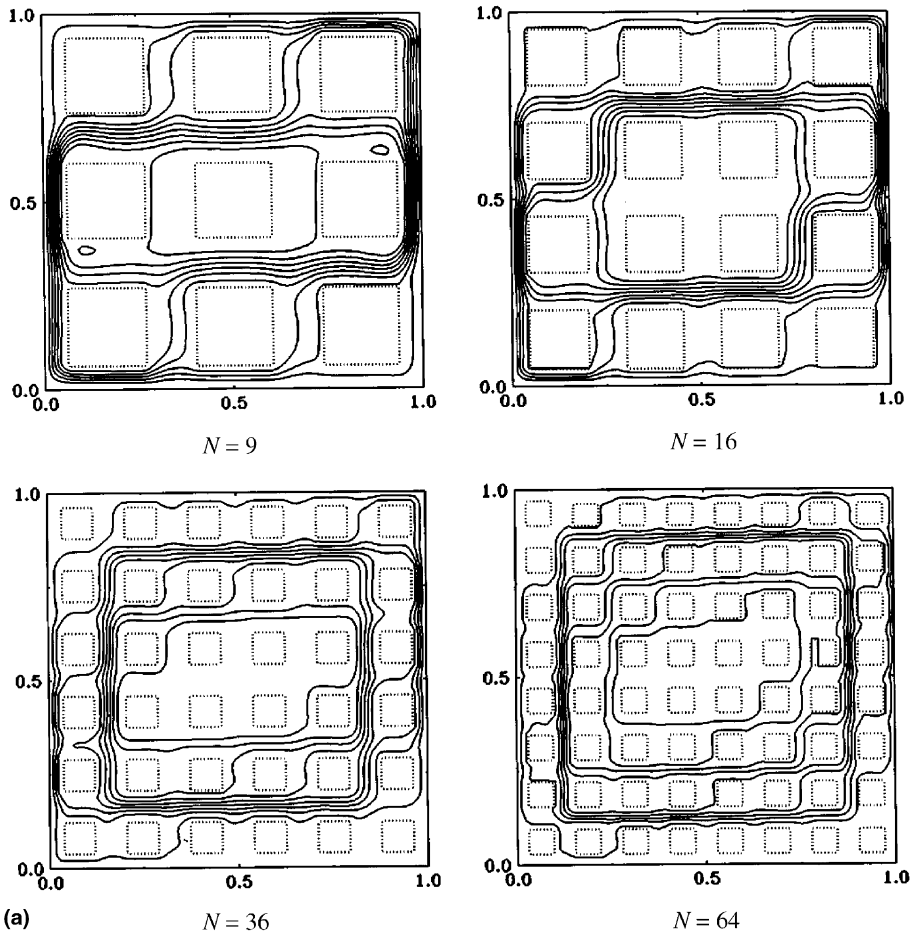

Fig. 2. Streamlines for: (a) $Ra = 10^6$, $\kappa = 1$; (b) $Ra = 10^7$, $\kappa = 1$.

outcome of becoming restricted to an effective shorter length of the heated (or cooled) wall.

Fig. 2b presents similar results for $Ra = 10^7$. Here the flow remains adjacent to the hot (and cold) wall even when $N = 36$. Although restraining flow effect caused by the proximity of the blocks to the walls is expected in this case, the higher Ra yields a narrower buoyancy region (closer to the walls), hindering the flow path switch phenomenon. This certainly affects flow structure along the horizontal adiabatic surfaces of the enclosure, with a relatively stronger flow observed when Ra is high for the same number of blocks, N.

Because the results of Fig. 2 are pertinent to $\kappa = 1$, effect of obstacles on the temperature distribution is expected to reflect, faithfully, their influence on the flow. Fig. 3a and Fig. 3b demonstrate the isothermal distribution corresponding to the streamlines shown in Fig. 2, for $Ra = 10^6$ and 10^7, respectively. For the case $Ra = 10^6$, observe how the isotherms along the hot (left) wall, from bottom to top, progressively shift further away from the wall as N increases. The waviness of the isotherms observed mainly near the hot and cold walls reflects flow channeling in between the blocks as observed in Fig. 2. As N increases, isotherms tend to stand parallel to the vertical walls indicating a reduction in the flow intensity within the enclosure. The isotherms of Fig. 3b, for high Ra, show the characteristic vertical temperature stratification away from the walls.

From Figs. 2 and 3, the blocks seem to have a hindering effect on the flow as N increases, with this effect being more pronounced when the buoyancy region adjacent to the hot and cold walls is wider, or equivalent to the case of low Ra. This observation is corroborated by Fig. 4, which exhibits Nu_{av} evolution as N increases. Observe the Nu_{av} variation with N that switches as Ra increases from 10^6 to 10^7, for instance. For $Ra = 10^7$, Nu_{av} decreases by only 5.2% when N increases from 9 to 16; however, when $Ra = 10^6$ the decrease is over 31%. For

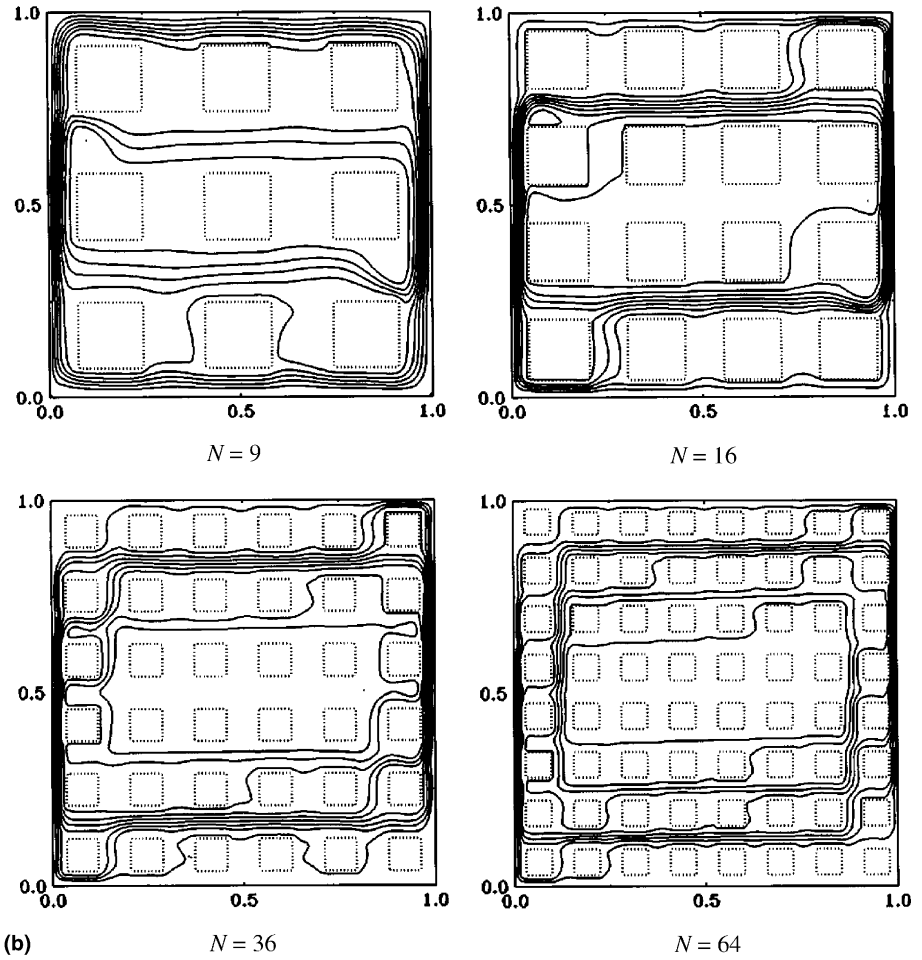

Fig. 2 (*continued*)

$Ra = 10^8$, the Nu_{av} decay is appreciable only when N increases from 64 to 144 due to the very narrow buoyancy region achieved for such a high Ra.

An analytical prediction for the flow switch explained above can be obtained by comparing the estimated scale of the boundary layer along a heated (or cooled) channel wall to the space between the wall and the blocks in the enclosure. From Bejan [10], p. 365, for a $Pr \geqslant 1$ fluid, the boundary layer is confined to the entire space between two isothermal walls when $Ra^{-1/4} = S^*$, where S^* is the non-dimensional distance between the two walls. For a single heated wall, $Ra^{-1/4} = S^*/2$ is a better scale. The distance, S, available for the fluid to flow in between the heated (or cooled) wall and the first column of blocks in the present case can be estimated as $S = (1 - DN^{1/2})/(2N^{1/2})$, or $S = (1 - \gamma^{1/2})/(2N^{1/2})$. One would expect the fluid to channel away from the wall only when the boundary layer (region of buoyancy effect) grows beyond the space between the wall and the first column of blocks, i.e., when $S^* > S$, or when

$$N > \frac{(1-\gamma^{1/2})^2}{16} Ra^{1/2} \tag{13}$$

In the present study $\gamma = 0.36$, so using Eq. (13) the minimum number of blocks required for flow switch becomes:

$$N_{\min} = 0.01 Ra^{1/2} \tag{14}$$

Hence, the fluid will only channel away from the heated (or cooled) wall when N is greater than (or $N_{\min}$ equals to) 3, 10, 32, 100, and 316, for $Ra = 10^5$, 10^6, 10^7, 10^8, 10^9, respectively. In this case, one would expect Nu_{av} to decrease as N increases. When $N < N_{\min}$, flow will remain between the first column of blocks and the vertical walls, so the effect of increasing the number of blocks (or N) on the heat transfer process should be minor. Results predicted by Eq. (14) are included

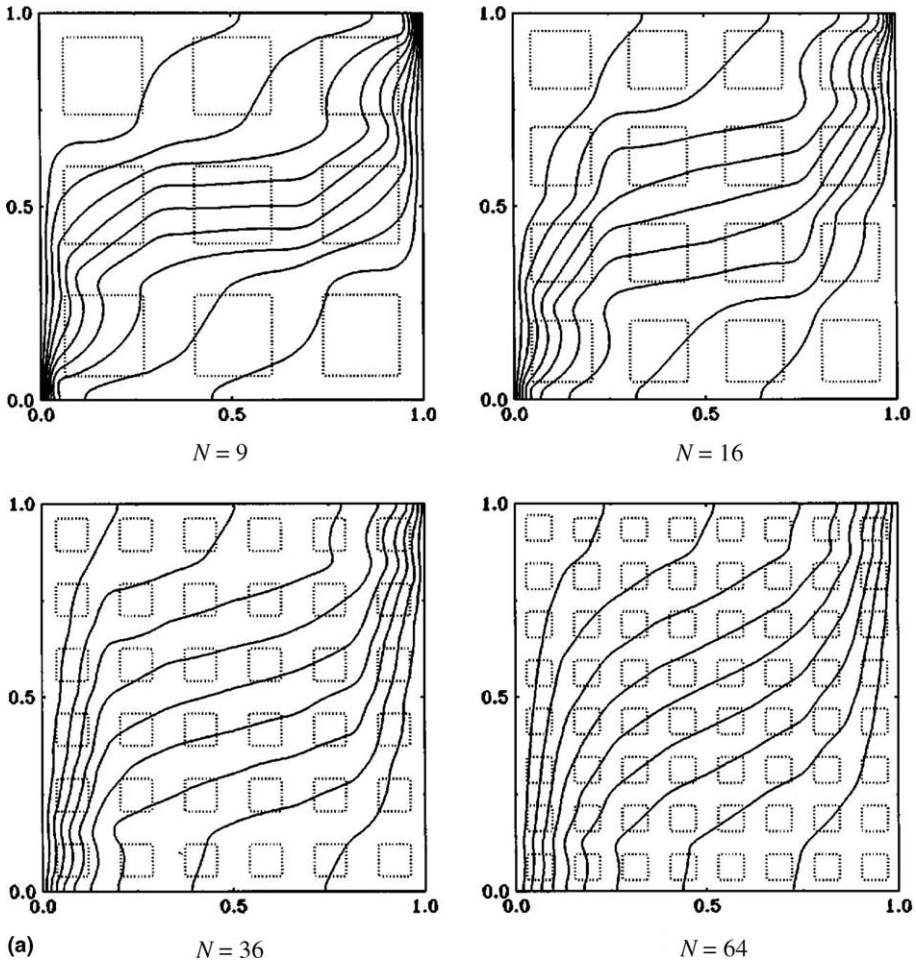

Fig. 3. (a) Isotherms for $Ra = 10^6$, $\kappa = 1$; (b) $Ra = 10^7$, $\kappa = 1$.

graphically in Fig. 4: for each Ra value, N_{min} predicted by Eq. (14) becomes the one marked by the intersection between the dashed line with the Ra curves. Observe that, to the right of the dashed line, $N > N_{min}$ indicating that Nu_{av} decreases with an increase in N. This prediction is confirmed well by the numerical results.

The effect of the solid–fluid thermal conductivity ratio κ on the flow field and heat transfer process is more difficult to predict because of two competing effects. For a fixed block distribution, when $\kappa > 1$, the solid blocks near the hot or cold walls will increase the heat transfer from the wall and, by consequence, widen the effective buoyancy region, enhancing the convective process. This effect should be more prevalent when Ra is low because the original buoyancy region (thermal boundary layer thickness) is wide in this case so that the blocks adjacent to the wall become active participants of the heat transfer process. However, the blocks located away from the walls should also enhance the heat transfer rate from the top horizontal fluid stream to the bottom horizontal fluid stream, hindering the overall heat transfer process (vertical conduction).

For $\kappa < 1$ and small Ra the opposite will take place, i.e., convection along the walls will be restrained to a narrower region and the vertical heat transfer within the mid-section of the enclosure between top and bottom horizontal fluid streams (vertical conduction) will be hindered. Also, the κ effect on the convection process should be minor when Ra is high.

The validation of the above predictions can be verified by considering Fig. 5, in which streamlines (5a) and their corresponding isotherms (5b) are plotted for $Ra = 10^6$ and $N = 36$, and for $\kappa = 0.1,1$, and 10. Based on the results of Fig. 4, the configuration yields a wide buoyancy region; the blocks adjacent to the wall participate actively on the heat transfer process. It is clear from Fig. 5a that more fluid is set to flow far from the heated (or cooled) wall as κ increases. At the same time,

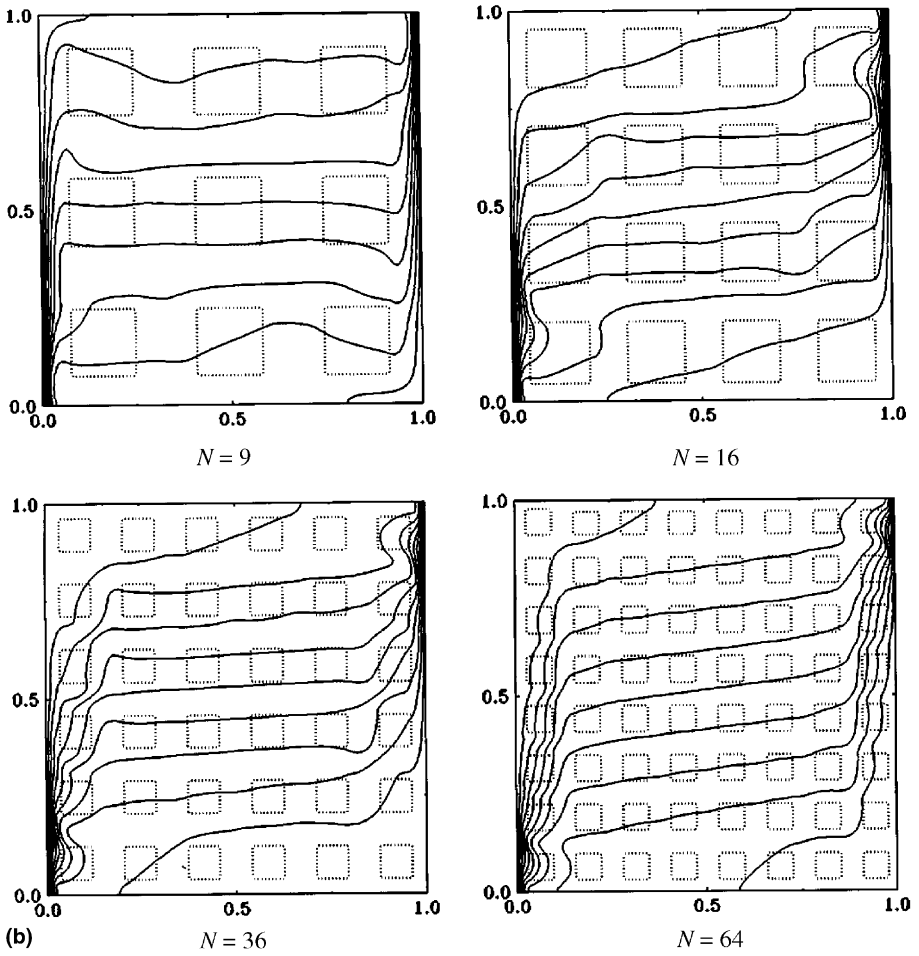

Fig. 3 (*continued*)

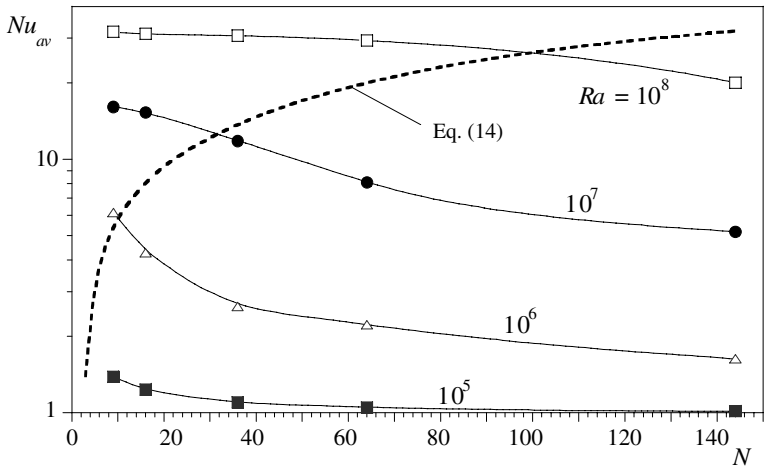

Fig. 4. Average Nusselt number versus the number of blocks for various *Ra*. Dashed line shows results predicted by Eq. (14).

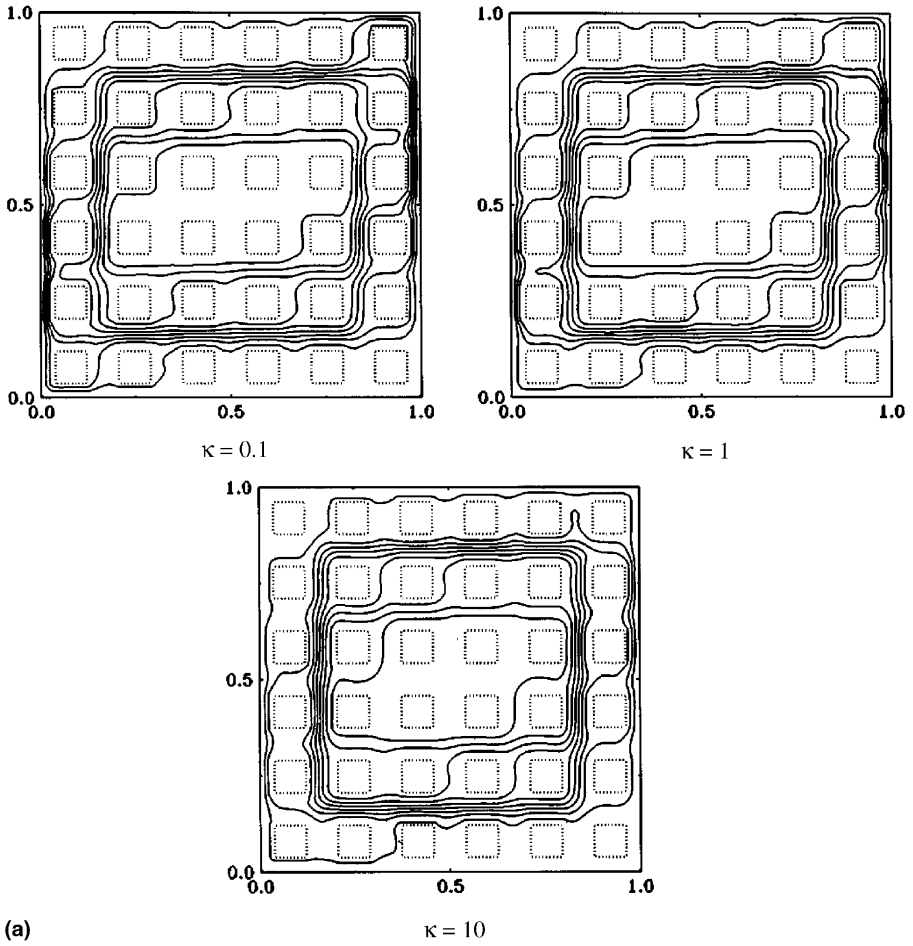

Fig. 5. Streamlines for: (a) $Ra = 10^6$, $N = 36$; (b) $Ra = 10^6$, $N = 36$.

from Fig. 5b, the stratification within the center of the enclosure seems to hold as κ increases. The net effect should yield an increase in Nu_{av} as κ increases.

The above conjecture is confirmed by Fig. 6, where results are presented for $N = 36$ and $Ra = 10^6$. Interesting is the behavior of the curve for $Ra = 10^7$ and $N = 36$ included in the same graph. Even though only slightly, in this case, the effect of increasing κ is similar to that of reducing Nu_{av}. The difference is easy to explain by recalling that when $N = 36$ and $Ra = 10^6$ the buoyancy region extends away from the channel in between the wall and the first column of blocks. However, for the same number of blocks, when $Ra = 10^7$, the buoyancy region is limited to the channel between the wall and the first column of blocks. In this particular case, the effect of increasing κ is limited to the reduced thermal stratification within the center of the enclosure that yields a hindered Nu_{av}. This is corroborated by the curve $Ra = 10^7$ and $N = 64$ also included in the same figure, indicating an increase in Nu_{av} as κ increases; for Ra, $N = 64$ a buoyancy region wide enough to activate the first column of blocks is created.

Figs. 7 and 8 show the variation of Nu_{av} versus N for the low and high Ra values, respectively. In Fig. 7, observe the increase in Nu_{av} for both cases as κ increases. The results for $Ra = 10^6$ indicate that the effect of increasing κ becomes more pronounced when N increases beyond minimum N required for flow switch, i.e., for cases in which the buoyancy region extends itself away from the channel adjacent to the heated (or cooled) wall. Observe also how the curves invert their positions when N decreases from 16 to 9: the results for the lowest κ yield highest Nu_{av} for $N = 9$. In Fig. 8, for high Ra cases of 10^7 and 10^8, the effect of varying κ is much stronger when N is higher than the minimum N required for flow switch. Moreover, the inversion of the curves as N crosses the line of Eq. (14) is visible in both cases. Table 4 summarizes the numerical results.

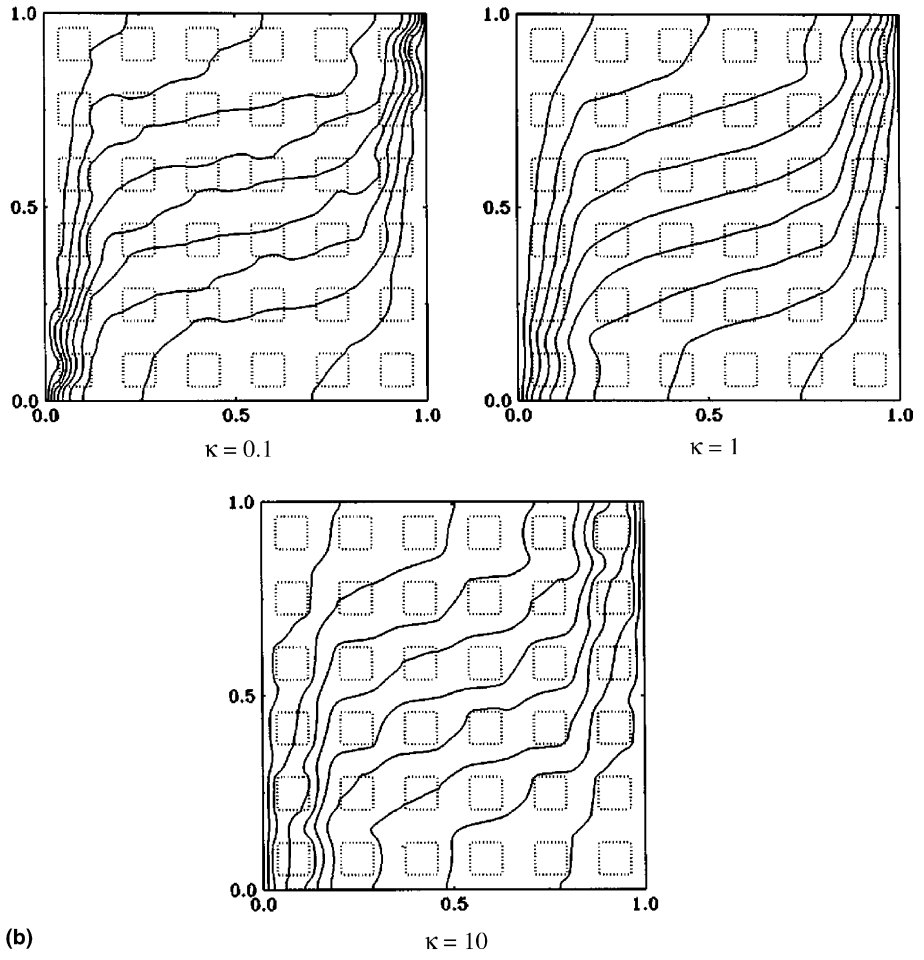

Fig. 5 (*continued*)

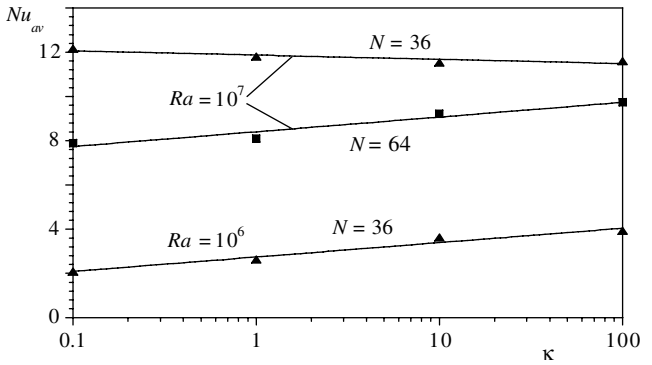

Fig. 6. The effect of varying κ on the average Nusselt number for $N = 36$ and 64.

4. Summary and conclusions

Natural convection within a differentially heated heterogeneous square enclosure consisting of several disconnected and conducting solid blocks within a saturated fluid is studied numerically. The amount of solid constituent within the enclosure is kept constant by fixing the solid-to-fluid volume ratio at 36%. Fluid

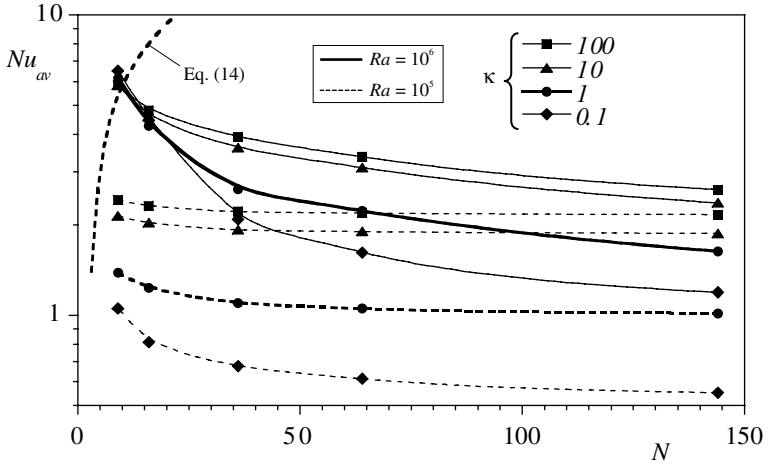

Fig. 7. The effect of varying κ on the average Nusselt number versus the number of blocks, for $Ra = 10^5$ and 10^6.

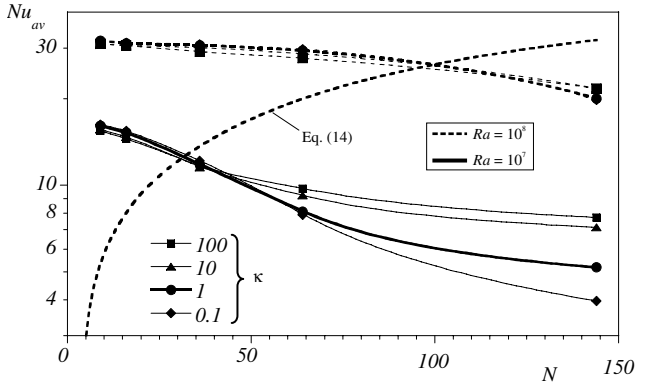

Fig. 8. The effect of varying κ on the average Nusselt number versus the number of blocks for $Ra = 10^7$ and 10^8.

Prandtl number is set as unity. The study covers Rayleigh number (Ra) from 10^5 to 10^8 and fluid-to-solid thermal conductivity ratio, κ from 0.1 to 100.

Results for $\kappa = 1$ indicate a switch from the fluid flowing predominantly along the channel between the heated (or cooled) enclosure wall and the first column of solid blocks, to the fluid flow penetrating on to the interior channels of the enclosure away from the heated (or cooled) wall as number of blocks increases. This phenomenon causes a drastic decrease in the heat transfer within the enclosure, and this decrease seems to be more pronounced (abrupt) at lower Ra.

Scale analysis argument provides means to derive an analytical expression for the minimum number of blocks necessary for the flow switch to take place. This analytical prediction, when compared to the numerical results, is proven to be exceptionally accurate, indicating that heat transfer across the enclosure is hindered when the number of solid blocks inside the enclosure is less than the minimum number necessary for the flow to switch, $N_{\min}$, for high fluid-to-solid thermal conductivity ratio, κ.

For a number of solid blocks bigger than the minimum number necessary for flow switch, $N_{\min}$, the heat transfer across the enclosure is enhanced as the fluid-to-solid thermal conductivity ratio κ increases; the effect of increasing κ becomes much more pronounced in this case. However, for $N < N_{\min}$ the degree of enhancement is inversely proportional to the Rayleigh number. Hence, the lowest κ would yield higher heat transfer

Table 4
Average Nusselt number, Nu_{av}, for various Ra, N, and κ

Ra	N	κ			
		0.1	1	10	100
10^5	9	1.053	*1.383*	2.140	2.418
	16	0.813	*1.233*	2.030	2.313
	36	0.676	*1.098*	1.922	2.211
	64	0.613	*1.051*	1.898	2.189
	144	0.551	*1.013*	1.873	2.162
10^6	9	6.526	*6.164*	5.835	5.833
	16	4.453	*4.274*	4.584	4.816
	36	2.089	*2.626*	3.616	3.929
	64	1.616	*2.223*	3.099	3.367
	144	1.191	*1.632*	2.366	2.619
10^7	9	16.253	*16.087*	15.661	15.475
	16	15.487	*15.258*	14.727	14.509
	36	12.161	*11.798*	11.540	11.606
	64	7.893	*8.094*	9.218	9.738
	144	3.963	*5.181*	7.146	7.726
10^8	9	31.816	*31.797*	31.056	31.035
	16	31.353	*31.180*	30.676	30.622
	36	30.904	*30.689*	30.115	29.133
	64	29.745	*29.394*	28.678	27.672
	144	19.792	*20.040*	21.710	21.710

for $N < N_{min}$. In general, the effect of increasing κ is that of enhancing the overall heat transfer process for $N > N_{min}$.

References

[1] A.A. Merrikh, A.A. Mohamad, Blockage effects in natural convection in differentially heated enclosures, J. Enhanc. Heat Transfer 8-1 (2001) 55–72.

[2] A.A. Merrikh, J.L. Lage, A.A. Mohamad, Natural convection in non-homogeneous heat generating media: comparison of continuum and porous-continuum models, J. Porous Media, in press.

[3] S.V. Patankar, Numerical Heat Transfer and Fluid Flow, Hemisphere, Washington DC, 1980.

[4] B.P. Leonard, A stable and accurate convective modeling procedure based on quadratic upstream interpolation, Comput. Methods Appl. Mech. Eng. 19 (1979) 59–98.

[5] J.M. House, C. Beckermann, T.F. Smith, Effect of a centered conducting body on natural convection heat transfer in an enclosure, Numer. Heat Transfer, Part A 18 (1990) 213–225.

[6] G. de Vahl Davis, Natural convection of air in a square cavity: a bench mark numerical solution, Int. J. Numer. Methods Fluids 3 (1983) 249–264.

[7] M. Hortmann, M. Peric, G. Sheuerer, Finite volume multigrid prediction of laminar natural convection: benchmark solutions, Int. J. Numer. Methods Fluids 11 (1990) 189–207.

[8] J.C. Kalita, D.C. Dalal, A.K. Dass, Fully compact higher-order computation of steady-state natural convection in a square cavity, Phys. Rev. E64 (066703) (2001) 1–13.

[9] J.L. Lage, A. Bejan, The *Ra–Pr* domain of laminar natural convection in an enclosure heated from the side, Numer. Heat Transfer, Part A 19 (1991) 21–41.

[10] A. Bejan, Convection Heat Transfer, second ed., John Wiley & Sons Inc., 1995.